Spectrochimica Acta Part A: Molecular and Biomolecular Spectroscopy 192 (2018) 458–463

Contents lists available at ScienceDirect

Spectrochimica Acta Part A: Molecular and Biomolecular Spectroscopy

journal homepage: www.elsevier.com/locate/saa

FTIR and Raman spectroscopic studies of selenium nanoparticles synthesised by the bacterium *Azospirillum thiophilum*

Anna V. Tugarova, Polina V. Mamchenkova, Yulia A. Dyatlova, Alexander A. Kamnev *

Laboratory of Biochemistry, Institute of Biochemistry and Physiology of Plants and Microorganisms, Russian Academy of Sciences, 13 Prosp. Entuziastov, 410049 Saratov, Russia

ARTICLE INFO

Article history:
Received 17 September 2017
Received in revised form 8 November 2017
Accepted 22 November 2017
Available online 23 November 2017

Keywords:
Selenium nanoparticles
Selenite reduction
Green chemistry
Azospirillum thiophilum
FTIR spectroscopy
Raman spectroscopy

ABSTRACT

Vibrational (Fourier transform infrared (FTIR) and Raman) spectroscopic techniques can provide unique molecular-level information on the structural and compositional characteristics of complicated biological objects. Thus, their applications in microbiology and related fields are steadily increasing. In this communication, biogenic selenium nanoparticles (Se NPs) were obtained via selenite (SeO_3^{2-}) reduction by the bacterium *Azospirillum thiophilum* (strain VKM B-2513) for the first time, using an original methodology for obtaining extracellular NPs. Dynamic light scattering (DLS) and transmission electron microscopy (TEM) showed the Se NPs to have average diameters within 160–250 nm; their zeta potential was measured to be minus 18.5 mV. Transmission FTIR spectra of the Se NPs separated from bacterial cells showed typical proteinacious, polysaccharide and lipid-related bands, in line with TEM data showing a thin layer covering the Se NPs surface. Raman spectra of dried Se NPs layer in the low-frequency region (under 500 cm^{-1} down to 150 cm^{-1}) showed a single very strong band with a maximum at 250 cm^{-1} which, in line with its increased width (ca. 30 cm^{-1} at half intensity), can be attributed to amorphous elementary Se. Thus, a combination of FTIR and Raman spectroscopic approaches is highly informative in non-destructive analysis of structural and compositional properties of biogenic Se NPs.

1. Introduction

Vibrational (Fourier transform infrared (FTIR) and Raman) spectroscopic techniques represent a well-established complementary and highly informative analytical arsenal, which has been successfully used in biology, particularly in microbiology and related fields, for studying samples of various complexity, from simple organic and biological molecules to supramolecular biosystems, cells and tissues (see, e.g. representative reports [1–11] and references cited therein). In our previous studies [12–19], FTIR and Raman spectroscopic techniques were used to monitor molecular-level changes in the structure and composition of cellular macrocomponents that accompanied metabolic responses of different strains of the ubiquitous rhizobacterium *Azospirillum brasilense* [20,21] (which showed different adaptation capabilities and often different ecological behaviour) to various stress conditions.

As was concluded in our recent review [22], vibrational spectroscopic techniques can also be useful in studying microbially synthesised selenium nanoparticles (Se NPs), FTIR spectroscopy being indispensible for analysing the bioorganic surface-associated components whereas Raman spectroscopy being sensitive to differences in various allotropic modifications and crystallinity of selenium in Se NPs.

The genus *Azospirillum* includes more than 15 species of bacteria which occupy different ecological niches [20,21]. For the first time for azospirilla, it has been shown [23,24] that *A. brasilense* (strains Sp245 and Sp7), a ubiquitous and most widely studied phytostimulating rhizobacterium of the genus *Azospirillum*, can reduce selenite (SeO_3^{2-}) to elementary selenium (Se^0) in the form of Se NPs (nanospheres, 50–400 nm in size). The ability of bacteria to reduce selenium oxyanions to elementary Se^0, besides possible nanobiotechnological applications of the biogenic Se NPs, can be promising for bioremediation of excessively selenium-rich soils and aquifers [22–26].

Using strain *A. brasilense* Sp7, a scheme has recently been developed for the synthesis of extracellular Se NPs more homogeneous in size (around 90 nm in diameter); their zeta potentials were determined, and the Se NPs obtained were characterised by FTIR spectroscopy [27]. In particular, Se NPs separated from bacterial cells showed FTIR bands of proteins, polysaccharides and lipids associated with the particles (in line with their TEM images which showed a thin layer over the NPs), in addition to strong carboxylate bands, which evidently stabilised the NP structure and morphology [27].

In this study, biogenic selenium nanoparticles (Se NPs) were obtained via selenite (SeO_3^{2-}) reduction by another species of *Azospirillum* (isolated from a sulphide-containing spring), *A. thiophilum* (strain

* Corresponding author.
E-mail addresses: aakamnev@ibppm.ru, a.a.kamnev@mail.ru (A.A. Kamnev).

https://doi.org/10.1016/j.saa.2017.11.050
1386-1425/

VKM B-2513) [28], for the first time, using the original methodology [27] for obtaining extracellular NPs. The resulting Se NPs isolated from the bacterial cells were characterised by dynamic light scattering (DLS) and transmission electron microscopy (TEM), as well as by FTIR and Raman spectroscopic techniques.

2. Materials and Methods

2.1. Bacterial Strain and Growth Conditions

Strain *Azospirillum thiophilum* VKM B-2513 [28] was taken from The Collection of Rhizosphere Microorganisms [WDCM 1021], according to the World Federation of Culture Collections, http://www.wfcc.info/ccinfo/collection/by_id/1021 maintained at the Institute of Biochemistry and Physiology of Plants and Microorganisms, Russian Academy of Sciences, Saratov, Russia. Bacteria were cultivated in a liquid modified malate salt medium (MSM) [29] which contained the following salts ($g \cdot l^{-1}$): K_2HPO_4, 3.0; KH_2PO_4, 2.0; NH_4Cl, 0.5; NaCl, 0.1; $FeSO_4 \cdot 7H_2O$, 0.02 (added as chelate with nitrilotriacetic acid); $CaCl_2$, 0.02; $MgSO_4 \cdot 7H_2O$, 0.2; $Na_2MoO_4 \cdot 2H_2O$, 0.002; sodium malate, 5.0 (obtained by mixing 3.76 g of malic acid with 2.24 g NaOH per litre), yeast extract, 0.1; final pH 6.8–7.0.

The culture (volume 100 ml in 250-ml Erlenmeyer flasks) was grown under aerobic conditions on a shaker (180 rpm) for up to 18–20 h at 28° C. Cell growth was monitored at $\lambda = 595$ nm (Spekol 221, Germany); the optical density (A_{595}) values of the resulting culture suspensions were about 0.7–0.8 (optical thickness 1 cm).

2.2. Bacterial Synthesis of Se NPs and Their Purification

Se NPs were synthesised by the strain *A. thiophilum* VKM B-2513 using the scheme reproduced for this bacterium species from our earlier work [27], in the presence of 5 mM Na_2SeO_3. All the next steps were performed under sterile conditions. Bacterial cells were harvested by centrifugation in 2-ml Eppendorf tubes (Minispin centrifuge; 15 min, 7000*g*) and washed three times with sterile saline solution (0.85% NaCl aqueous solution) to remove the culture medium components and extracellular components or bacterial exudates. The resulting wet biomass pellet was resuspended in half of the initial volume of sterile saline solution. Sodium selenite ($Na_2SeO_3 \cdot 5H_2O$, "Merck") as a 0.5 M stock aqueous solution was added to the suspensions up to a final concentration of 5 mM. Suspensions containing the cells (washed as above) and selenite were placed in a thermostat (at 31–32 °C). The culture of the same cell density without sodium selenite was used as a control. The process of SeO_3^{2-} reduction was monitored by colour change of the bacterial suspension from colourless to reddish [24]. The Se NPs formed therein and their localisation were monitored by transmission electron microscopy (TEM; see below).

After 24 h, the bacterial cells were removed from the suspension by 'soft' centrifugation (1400*g*, 5 min); the supernatant with Se NPs was collected and filtered through a 0.22 or 0.44 μm PVDF filter to remove occasional bacterial cells. The suspensions of Se NPs were further centrifuged at 12000*g* for 30 min, and the collected precipitate pellet was resuspended in a minimum volume of MilliQ water. The Se NPs obtained were characterised by TEM as well as by FTIR and Raman spectroscopic techniques (see below).

2.3. Transmission Electron Microscopy (TEM)

Samples of bacterial cells (after cultivation for 24 h with 5 mM selenite before centrifugation) or Se NPs (obtained and isolated as described above) were placed onto nickel or copper grids coated with formvar (1% formvar in 1,2-dichloroethane). TEM images were registered on a Libra-120 transmission electron microscope (Carl Zeiss, Jena, Germany).

2.4. Dynamic Light Scattering (DLS) and Zeta Potentials of Se NPs

The sizes of the bacterially synthesised Se NPs (using DLS) and their zeta potentials were measured on a Zetasizer Nano-ZS particle sizer and zeta potential analyzer (Malvern Instruments Ltd., Malvern, UK).

2.5. Fourier Transform Infrared (FTIR) Spectroscopy

For transmission FTIR measurements, the aqueous suspensions of Se NPs (isolated and purified as described above) were placed as thin films on clean flat ZnSe discs (CVD-ZnSe, "R'AIN Optics", Dzerzhinsk, Russia; diameter 2.5 cm, thickness 0.2 cm) and dried in a thermostatted desiccator at 45 °C.

Infrared spectroscopic measurements were performed on a Nicolet 6700 FTIR spectrometer (Thermo Electron Corporation, USA; DTGS detector; KBr beamsplitter). Spectra were collected in the transmission mode with a total of 64 scans (resolution 2 cm^{-1}) against the ZnSe disc background and manipulated using the OMNIC (version 8.2.0.387) software supplied by the manufacturer of the spectrometer. All spectra were smoothed using the standard "automatic smooth" function of the software which uses the Savitsky-Golay algorithm (95-point moving second-degree polynomial), and then the baseline was corrected using the "automatic baseline correct" function. All the FTIR spectroscopic measurements were repeated two or three times for each sample and were well reproducible.

2.6. Raman Spectroscopy

For Raman spectroscopic measurements, the aqueous suspensions of Se NPs (obtained as described in Subsection 2.2) were placed as thin films on small pieces of aluminium foil and dried in air at ambient temperature. Normal Raman spectra were acquired with a Peak Seeker Pro 785 Raman spectrometer (Ocean Optics) using 785 nm excitation (30 mW; spectral range 150–2100 cm^{-1}). The acquisition interval was 10 s, and all spectra were averaged over 10 independent runs. The acquired digital experimental spectroscopic data were processed and plotted by using Microsoft Excel 2010.

3. Results and Discussion

3.1. General Considerations

For *Azospirillum thiophilum* (strain VKM B-2513), we utilised the original scheme developed earlier for the synthesis of extracellular Se NPs [27]. Thus, in this work, extracellular Se NPs were synthesised for the first time by the *A. thiophilum* species in the presence of 5 mM Na_2SeO_3. The recently described bacterium *A. thiophilum* had been isolated from a sulphur-containing bacterial mat collected from a sulphide spring [28]. Thus, one of the aims in this study was to check whether this species can produce pure Se^0 in the form of Se NPs in the course of selenite reduction (vide infra). Note that there were indications in the literature that biogenic Se NPs produced, e.g. by methane-oxidising bacteria contained trace admixtures of sulphur, and the elemental maps of selenium and sulphur visualised by energy-dispersive X-ray spectroscopy (EDXS) for those Se NPs overlapped [30]. In addition, sulphur and selenium were reported to co-precipitate in the presence of sulphate-reducing bacteria [31] and in sulphur-accumulating bacteria [32].

3.2. TEM and DLS Studies

The Se NPs obtained in this work were separated including the removal of bacterial cells by centrifugation and filtration, purified by triple washing in Milli-Q water and concentrated. Typical transmission electron microscopic (TEM) images of the bacterial cells (incubated in saline solution for 24 h), after 24 h with 5 mM SeO_3^{2-} (before centrifugation),

and of purified Se NPs are presented in Fig. 1A and B, respectively. As can be seen, the Se NPs obtained were relatively uniform in size (as compared to those obtained as described in [24]). The Se NPs were characterised using DLS, and their calculated size distribution is presented in Fig. 1C. Note that the results of size measurements by DLS correspond to the TEM data (see Fig. 1A–B).

The results obtained show that the scheme for the bacterial synthesis of extracellular Se NPs proposed in [27] is applicable, at least, for other *Azospirillum* species.

The measured values of zeta potentials of these Se NPs were found to be −18.5 mV. Similar negative values of zeta potentials were reported earlier for biogenic Se NPs synthesised by other microorganisms [33–35]. This value is also close to (although slightly lower than) those determined by us for smaller (50–90 nm in diameter) Se NPs synthesised by a strain of another *Azospirillum* species, *A. brasilense* Sp245, which were –(21…24) mV (A.V. Tugarova, P.V. Mamchenkova, A.A. Kamnev, unpublished results). Negative values of zeta potentials are evidently related to the presence of negatively charged functional groups at the NPs surface. According to the recent literature [33–35], bacterially synthesised Se NPs may be covered by a layer containing various bio(macro)molecules, including proteins and/or polysaccharides, that govern their surface charge [34]. Similar data about a surface-associated composite carboxylate-containing bioorganic layer were reported for Se NPs synthesised by *A. brasilense* strain Sp7 [27] (see below).

3.3. Vibrational Spectroscopic Studies

3.3.1. FTIR Spectroscopy

The obtained Se NPs were further characterised by vibrational spectroscopic techniques. Fig. 2 shows a typical FTIR spectrum (registered in the transmission mode) of the Se NPs produced by *A. thiophilum* VKM B-2513 (separated and purified as described in the experimental section). The wavenumbers of the maxima for the main bands in the FTIR spectrum in Fig. 2 are summarised in Table 1 together with their assignment based on the data reported earlier [3–5,7,17,27,36,37].

FTIR spectra of the purified Se NPs clearly show the presence of various capping biomacromolecules at the Se NPs surface (note that in their TEM image illustrated by Fig. 2B, a thin layer between adjoining NPs is clearly visible). The typical protein bands, amide I (which is split, with two maxima at 1656 and 1635 cm^{-1}, that could be attributed to the secondary structure with comparable presence of both α-helix and β-structured regions, respectively [3–5,17,36]), amide II (at 1542 cm^{-1}) and low-intensity amide III, can be clearly seen (see Table 1). Note

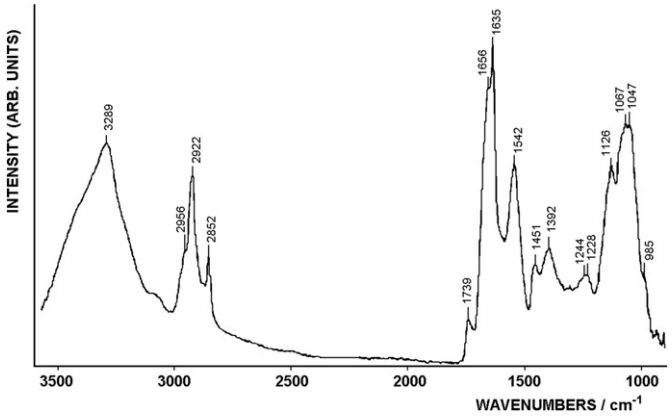

Fig. 2. Fourier transform infrared spectrum (in the transmission mode, measured as a dry thin layer on ZnSe disc) of SeNPs synthesised by *A. thiophilum* VKM B-2513 (incubated at 32 °C for 24 h in physiological saline with 5 mM Na_2SeO_3), separated from the cells and purified.

that the amide II band of proteins in this case can overlap and evidently mask the usually relatively strong carboxylate band $\nu_{as}(COO^-)$ (which was detected at 1565 cm^{-1} for Se NPs produced by *A. brasilense* Sp7 [27], but may appear at somewhat higher or lower frequencies [36]). The presence of carboxylate groups (besides the negative charge of the Se NPs; see subsection 3.2) is figured out from the appearance of the accompanying symmetric stretching $\nu_s(COO^-)$ band at 1392 cm^{-1}. The typical polysaccharide vibration region (within ca. 1200–1000 cm^{-1}) is also featured by very strong absorption (see Fig. 2 and Table 1), although the corresponding strong stretching C—O/C—C and bending C—O—H or C—O—C modes typical of polysaccharides can contain some contributions from similar functional groups in proteins and polyesters. These results clearly show the presence of proteins and polysaccharides in the biomacromolecules capping the Se NPs surface, in line with the TEM image (see Fig. 1B) and with the literature on biosynthesised Se nanostructures [33–35,38–40].

The presence of lipids in the capping layer of the obtained Se NPs is featured by the increased C—H stretching modes (within 3000–2800 cm^{-1}, with the dominating $\nu_{as}(CH_2)$ and $\nu_s(CH_2)$ bands corresponding to aliphatic chains of fatty-acid residues) with the accompanying weaker ν(C═O) band at 1739 cm^{-1} typical of ester moieties (see Fig. 2 and Table 1). These are virtually identical both in their positions and relative intensities to those observed earlier for Se NPs produced by *A. brasilense* Sp7 [27]. Note also that lipids have recently

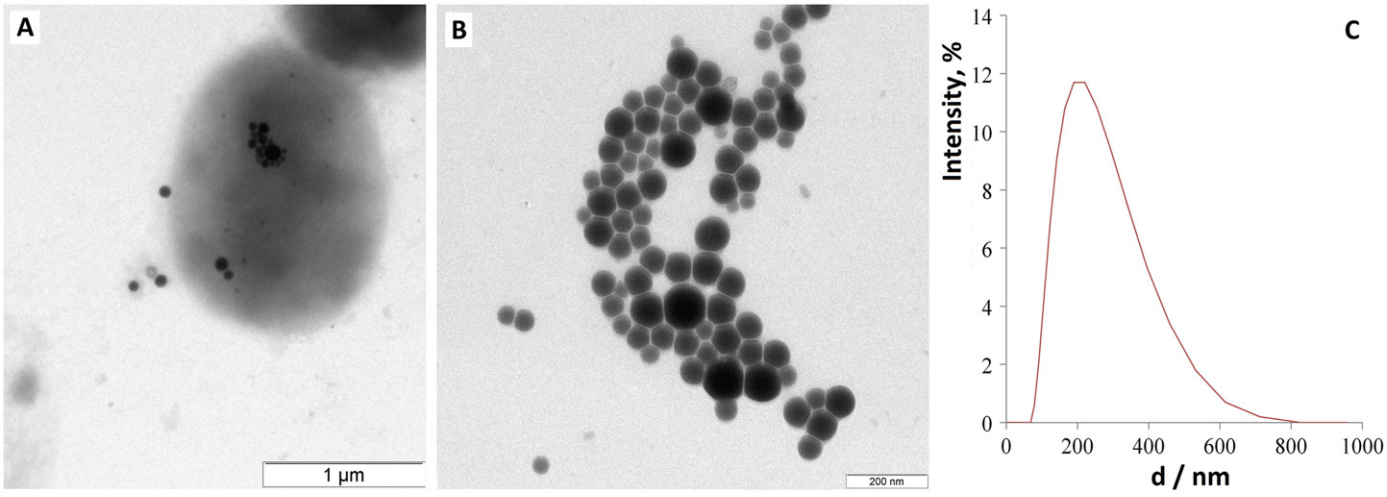

Fig. 1. Transmission electron microscopic images of *A. thiophilum* VKM B-2513, incubated for 24 h in the presence of 5 mM Na_2SeO_3 (A; bar: 1 μm); of isolated and purified Se NP (B; bar: 200 nm), as well as the size distribution (*d*, diameter of NPs) of the obtained Se NPs (calculated using DLS) (C).

Table 1
Wavenumbers of the main bands in the FTIR spectrum of Se NPs (see Fig. 2) and their assignment [3–5,7,17,27,36,37].

Assignment of main bands to the relevant functional groups (wavenumbers, cm^{-1})											
O–H; N–H (amide A in proteins), ν	C–H in $-CH_3$, ν_{as}	C–H in $>CH_2$, ν_{as}	C–H in $>CH_2$, ν_s	C═O (ester moiety), ν	Amide I (in proteins)	Amide II (in proteins)	$-CH_2/-CH_3$ δ (in proteins, lipids, polyesters, etc.)	COO^-, ν_s	Amide III/O–P═Oν_{as}	C–O, C–C ν, C–O–H, C–O–C δ in polysaccharides, proteins and polyesters	Phosphoryl group, ν_s
3289; ~3080 (sh)	2956[a] (w, sh)	2922	2852	1739 (w)	1656, 1635	1542	1451	1392[b]	1244, 1228 (w)	1126, 1067, 1047	985 (w)

Designations: ν – stretching vibrations; ν_s – symmetric stretching vibrations; ν_{as} – antisymmetric stretching vibrations; δ – bending vibrations; sh – shoulder; w – weak.
[a] The commonly less intense corresponding symmetric vibrations ν_s(C–H) of methyl groups (which, when resolved, appear at ca. 2874 cm^{-1}; see, e.g [27]) may in this case be masked by the stronger methylene modes $\nu_{as}(CH_2)$ at 2922 cm^{-1} and $\nu_s(CH_2)$ at 2852 cm^{-1} of aliphatic chains in lipids (see also Fig. 2).
[b] The intense amide II band (related to proteins) can mask the carboxylic $\nu_{as}(COO^-)$ band, which may be relatively weak here, considering the accompanying weaker $\nu_s(COO^-)$ band (observed at 1392 cm^{-1}).

been reported to be among biomacromolecular capping constituents of microbially produced Se NPs [38].

It has to be mentioned, however, that, according to the present spectroscopic results (see Fig. 2 and Table 1), in comparison with the earlier data on Se NPs produced by *A. brasilense* Sp7 [27], the content of carboxylic moieties in the biomacromolecular 'shell' of the Se NPs synthesised in this work by *A. thiophilum* VKM B-2513 is considerable lower (this corresponds to their lower zeta potential; vide supra). It may be ascribed to partial removal of carboxylate-containing constituents by additional washing of the NPs: in fact, in this work it was also found that the amount of carboxylic moieties contained in the biomacromolecular 'shell' can be noticeably decreased by washing. Thus, the carboxylate-containing components are likely to be relatively loosely bound to the Se NPs surface, in contrast to the biomacromolecular 'shell' itself which is rather stable. The reasons for the partial variability of the capping layer composition of these biogenic Se NPs evidently need to be further investigated.

3.3.2. Raman Spectroscopy

As was mentioned earlier (see Section 1), Raman spectroscopy is known to be sensitive to differences in various allotropic modifications and crystallinity of selenium [41,42], which is useful for studying Se nanomaterials. For Se NPs produced by *A. thiophilum* VKM B-2513, their Raman spectrum in the whole lower-frequency region (particularly, under 500 cm^{-1}) showed a single very strong band with a maximum at 250 cm^{-1} (Fig. 3) which corresponds to the A1 stretching Se—Se mode [41,42] and, in line with its increased half-width (ca. 30 cm^{-1}), can be attributed to amorphous Se [41–43]. It may be noted for

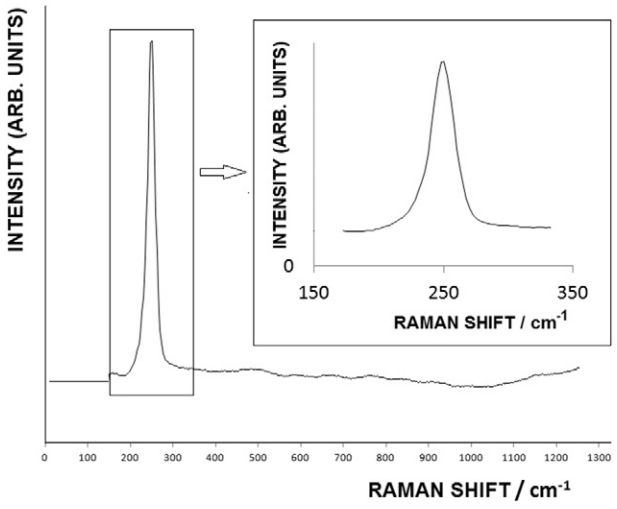

Fig. 3. Raman spectrum of SeNPs, synthesised by *Azospirillum thiophilum* VKM B-2513 (incubated with 5 mM of sodium selenite within 24 h), isolated from the bacterial cells and purified (inset: expanded region 150–350 cm^{-1}).

comparison that Raman spectra for Se NPs synthesised by *A. brasilense* Sp7 were analogous (data not shown).

The additional evidence for the lack of crystallinity of the Se NPs under study is the absence of any other clearly noticeable close (or overlapping) lower-frequency bands, besides that at 250 cm^{-1} (see Fig. 3). It is noteworthy that, according to Eysel and Sunder [44], in the Raman spectrum of pure polycrystalline selenium, along with a strong and narrow band of the stretching Se—Se mode at 251 cm^{-1}, there is a clearly seen shoulder at about 240 cm^{-1} (along with an equally strong narrow band at 111 cm^{-1} related to the skeleton deformation vibrations of Se_8 molecules; this region is out of our spectral range (see subsection 2.6)). (Very similar frequencies were reported by Lucovsky et al. [41] for an α-monoclinic selenium crystal). As for amorphous selenium (cast samples), Lucovsky et al. [41] mentioned that on the broadened Se_8-related Raman band at 250 cm^{-1} related to the stretching Se—Se vibration mode, there was a shoulder at 235 cm^{-1} (interpreted as being due to both E and A_1 stretch modes of the polymeric chain structure). In our case (see Fig. 3), there is no clearly visible shoulder in this region (which, under the resolution used, was also not revealed in the 2nd derivative of the spectrum; data not shown). This may point to some structural differences between biogenic amorphous Se NPs (such as those studied in our work) and cast samples of bulk amorphous selenium (studied in [41]), which requires further investigation.

In view of the data mentioned above (see Subsection 3.1) considering the presence of sulphur in some biogenic Se NPs [30–32], it is important to emphasize that the present straightforward Raman spectroscopic results provide evidence that the obtained amorphous Se NPs contained, besides the bioorganic 'shell', pure elementary selenium(0), as there are no signs of either stretching Se—S bonds (observed at ~352–377 cm^{-1}) or homonuclear stretching S—S bonds (observed within ca. 430–470 cm^{-1}) [44]. Note that in the very recent report by Vogel et al. [45], *Azospirillum brasilense* (strain Cd; DSMZ 1843 [46]) was shown to be capable of producing mixed Se—S extracellular particles of the average diameter about 400 nm with the composition close to Se_6S_2, which gave a strong broadened Raman Se—Se stretching band centred at 257 cm^{-1} and a weak but noticeable broadened band at 356 cm^{-1} ascribed to S—Se stretching vibrations [44,45]. In our case (see Fig. 3), however, we do not see any sulphur-related bands in the Raman spectrum (note that in the culture medium used in our experiments, sulphate ions were present at a concentration ca. 1 mM (see Subsection 2.1), although this is about an order of magnitude lower than that used by Vogel et al. [45] who added 1 $g \cdot l^{-1}$ $(NH_4)_2SO_4$ to the culture medium).

4. Conclusions

Extracellular selenium nanoparticles (Se NPs) were obtained via selenite (SeO_3^{2-}) reduction by the bacterium *Azospirillum thiophilum* (strain VKM B-2513) for the first time, using an original methodology (developed by the authors earlier and applied to another *Azospirillum* species, *A. brasilense*, strain Sp7 [27]). The Se NPs characterised by

dynamic light scattering (DLS) and transmission electron microscopy (TEM) had average diameters within 160–250 nm; their zeta potential was −18.5 mV. FTIR spectra of the biogenic Se NPs provided evidence for the presence of proteinaceous, polysaccharide and lipid-containing surface 'shell', in line with TEM data showing a thin layer covering the Se NPs surface. Raman spectra of dried Se NPs layer in the low-frequency region (under 500 cm^{-1}) showed a single very strong band with a maximum at 250 cm^{-1} which, in line with its increased width (ca. 30 cm^{-1} at half intensity), can be attributed to amorphous elementary Se. Thus, a combination of FTIR and Raman spectroscopic approaches is highly informative in non-destructive analysis of structural and compositional properties of biogenic Se NPs.

Acknowledgments

In this work, experiments were performed in part on the equipment of the "Simbioz" Centre for the Collective Use of Research Equipment in the field of physical–chemical biology and nanobiotechnology at this Institute, Saratov, Russia (Zetasizer Nano-ZS, FTIR spectrometer Nicolet 6700, transmission electron microscope Libra-120). The main materials of this paper were presented at the Colloquium Spectroscopicum Internationale XL (CSI XL; 11–16 June 2017, Pisa, Italy); A.V.T. acknowledges the support provided by the CSI XL Organising Committee for participating in the Congress. The authors are grateful to Dr. A.M. Burov (this Institute, Saratov, Russia) for his help in carrying out the transmission electron microscopic experiments and to D.Sc. B.N. Khlebtsov (this Institute, Saratov, Russia) for his help in carrying out Raman spectroscopic measurements. Thanks are also due to E.A. Polivoda (this Institute, Saratov, Russia) for her technical assistance with transmission electron microscopy.

This study was supported in part by The Russian Foundation for Basic Research (Grant 16-08-01302-a).

Conflict of Interest Statement

The authors declare that the research was conducted in the absence of any commercial or financial relationships that could be construed as a potential conflict of interest.

References

[1] P.D. Nichols, J.M. Henson, J.B. Guckert, D.E. Nivens, D.C. White, Fourier transform-infrared spectroscopic methods for microbial ecology: analysis of bacteria, bacteria-polymer mixtures and biofilms, J. Microbiol. Methods 4 (2) (1985) 79–94, https://doi.org/10.1016/0167-7012(85)90023-5.

[2] D. Naumann, S. Keller, D. Helm, Ch. Schultz, B. Schrader, FT-IR spectroscopy and FT-Raman spectroscopy are powerful analytical tools for the non-invasive characterization of intact microbial cells, J. Mol. Struct. 347 (1995) 399–405, https://doi.org/10.1016/0022-2860(95)08562-A.

[3] D. Naumann, Infrared spectroscopy in microbiology, in: R.A. Meyers (Ed.), Encyclopedia of Analytical Chemistry, Wiley, Chichester, UK 2000, pp. 102–131, https://doi.org/10.1002/9780470027318.a0117 (Updated version: P. Lasch, D. Naumann. Infrared spectroscopy in microbiology. In: R.A. Meyers (Ed.). Encyclopedia of Analytical Chemistry. J. Wiley & Sons. Published online 12 March 2015. https://doi.org/10.1002/9780470027318.a0117.pub2).

[4] M. Beekes, P. Lasch, D. Naumann, Analytical applications of Fourier transform infrared (FT-IR) spectroscopy in microbiology and prion research, Vet. Microbiol. 123 (4) (2007) 305–319, https://doi.org/10.1016/j.vetmic.2007.04.010.

[5] A.A. Kamnev, FTIR spectroscopic studies of bacterial cellular responses to environmental factors, plant-bacterial interactions and signalling, Spectrosc. Int. J. 22 (2–3) (2008) 83–95, https://doi.org/10.3233/SPE-2008-0329.

[6] D.R. Gauger, V.V. Andrushchenko, P. Bouř, W. Pohle, A spectroscopic method to estimate the binding potency of amphiphile assemblies, Anal. Bioanal. Chem. 398 (2) (2010) 1109–1123, https://doi.org/10.1007/s00216-010-3969-0.

[7] J.J. Ojeda, M. Dittrich, Fourier transform infrared spectroscopy for molecular analysis of microbial cells, in: A. Navid (Ed.), Microbial Systems Biology: Methods and Protocols (Methods in Molecular Biology, Vol. 881), Chapter 8, Springer, New York 2012, pp. 187–211, https://doi.org/10.1007/978-1-61779-827-6_8.

[8] G.A. Pitsevich, A.E. Malevich, E.N. Kozlovskaya, I.Yu. Doroshenko, V.E. Pogorelov, V. Sablinskas, V. Balevicius, Theoretical study of the C—H/O—H stretching vibrations in malonaldehyde, Spectrochim. Acta A Mol. Biomol. Spectrosc. 145 (2015) 384–393, https://doi.org/10.1016/j.saa.2015.02.067.

[9] Y. Du, H.X. Fang, Q. Zhang, H.L. Zhang, Z. Hong, Spectroscopic investigation on cocrystal formation between adenine and fumaric acid based on infrared and Raman techniques, Spectrochim. Acta A Mol. Biomol. Spectrosc. 153 (2016) 580–585, https://doi.org/10.1016/j.saa.2015.09.020.

[10] G. Güler, M.M. Vorob'ev, V. Vogel, W. Mäntele, Proteolytically-induced changes of secondary structural protein conformation of bovine serum albumin monitored by Fourier transform infrared (FT-IR) and UV-circular dichroism spectroscopy, Spectrochim. Acta A Mol. Biomol. Spectrosc. 161 (2016) 8–18, https://doi.org/10.1016/j.saa.2016.02.013.

[11] E.A. Kogkaki, M. Sofoulis, P. Natskoulis, P.A. Tarantilis, C.S. Pappas, E.Z. Panagou, Differentiation and identification of grape-associated black aspergilli using Fourier transform infrared (FT-IR) spectroscopic analysis of mycelia, Int. J. Food Microbiol. 259 (2017) 22–28, https://doi.org/10.1016/j.ijfoodmicro.2017.07.020.

[12] A.A. Kamnev, M. Ristic, L.P. Antonyuk, A.V. Chernyshev, V.V. Ignatov, Fourier transform infrared spectroscopic study of intact cells of the nitrogen-fixing bacterium *Azospirillum brasilense*, J. Mol. Struct. 408/409 (1997) 201–205, https://doi.org/10.1016/S0022-2860(96)09532-4.

[13] A.A. Kamnev, L.P. Antonyuk, L.Yu. Matora, O.B. Serebrennikova, M.V. Sumaroka, M. Colina, M.-F. Renou-Gonnord, V.V. Ignatov, Spectroscopic characterization of cell membranes and their constituents of the plant associated soil bacterium *Azospirillum brasilense*, J. Mol. Struct. 480–481 (1999) 387–393, https://doi.org/10.1016/S0022-2860(98)00712-1.

[14] A.A. Kamnev, P.A. Tarantilis, L.P. Antonyuk, L.A. Bespalova, M.G. Polissiou, M. Colina, P.H.E. Gardiner, V.V. Ignatov, Fourier transform Raman spectroscopic characterisation of cells of the plant-associated soil bacterium *Azospirillum brasilense* Sp7, J. Mol. Struct. 563-564 (2001) 199–207, https://doi.org/10.1016/S0022-2860(00)00877-2.

[15] A.A. Kamnev, L.P. Antonyuk, A.V. Tugarova, P.A. Tarantilis, M.G. Polissiou, P.H.E. Gardiner, Fourier transform infrared spectroscopic characterisation of heavy metal-induced metabolic changes in the plant-associated soil bacterium *Azospirillum brasilense* Sp7, J. Mol. Struct. 610 (1–3) (2002) 127–131, https://doi.org/10.1016/S0022-2860(02)00021-2.

[16] A.A. Kamnev, A.V. Tugarova, L.P. Antonyuk, P.A. Tarantilis, L.A. Kulikov, Yu.D. Perfiliev, M.G. Polissiou, P.H.E. Gardiner, Instrumental analysis of bacterial cells using vibrational and emission Mössbauer spectroscopic techniques, Anal. Chim. Acta 573-574 (2006) 445–452, https://doi.org/10.1016/j.aca.2006.04.041.

[17] A.A. Kamnev, J.N. Sadovnikova, P.A. Tarantilis, M.G. Polissiou, L.P. Antonyuk, Responses of *Azospirillum brasilense* to nitrogen deficiency and to wheat lectin: a diffuse reflectance infrared Fourier transform (DRIFT) spectroscopic study, Microb. Ecol. 56 (4) (2008) 615–624, https://doi.org/10.1007/s00248-008-9381-z.

[18] A.A. Kamnev, A.V. Tugarova, P.A. Tarantilis, P.H.E. Gardiner, M.G. Polissiou, Comparing poly-3-hydroxybutyrate accumulation in *Azospirillum brasilense* strains Sp7 and Sp245: the effects of copper (II), Appl. Soil Ecol. 61 (2012) 213–216, https://doi.org/10.1016/j.apsoil.2011.10.020.

[19] A.V. Tugarova, A.V. Scheludko, Yu.A. Dyatlova, Yu.A. Filip'echeva, A.A. Kamnev, FTIR spectroscopic study of biofilms formed by the rhizobacterium *Azospirillum brasilense* Sp245 and its mutant *Azospirillum brasilense* Sp245.1610, J. Mol. Struct. 1140 (2017) 142–147, https://doi.org/10.1016/j.molstruc.2016.12.063.

[20] L. Pereg, L.E. de Bashan, Y. Bashan, Assessment of affinity and specificity of *Azospirillum* for plants, Plant Soil 399 (1–2) (2016) 389–414, https://doi.org/10.1007/s11104-015-2778-9.

[21] F. Cassán, M. Diaz-Zorita, *Azospirillum* sp. in current agriculture: From the laboratory to the field, Soil Biol. Biochem. 103 (2016) 117–130, https://doi.org/10.1016/j.soilbio.2016.08.020.

[22] A.V. Tugarova, A.A. Kamnev, Proteins in microbial synthesis of selenium nanoparticles, Talanta 174 (2017) 539–547, https://doi.org/10.1016/j.talanta.2017.06.013.

[23] A.V. Tugarova, E.P. Vetchinkina, E.A. Loshchinina, A.G. Shchelochkov, V.E. Nikitina, A.A. Kamnev, The ability of the rhizobacterium *Azospirillum brasilense* to reduce selenium(IV) to selenium(0), Microbiology (Moscow) 82 (3) (2013) 352–355, https://doi.org/10.1134/S0026261713030120.

[24] A.V. Tugarova, E.P. Vetchinkina, E.A. Loshchinina, A.M. Burov, V.E. Nikitina, A.A. Kamnev, Reduction of selenite by *Azospirillum brasilense* with the formation of selenium nanoparticles, Microb. Ecol. 68 (3) (2014) 495–503, https://doi.org/10.1007/s00248-014-0429-y.

[25] A.S. Eswayah, T.J. Smith, P.H.E. Gardiner, Microbial transformations of selenium species of relevance to bioremediation, Appl. Environ. Microbiol. 82 (16) (2016) 4848–4859, https://doi.org/10.1128/AEM.00877-16.

[26] L.S. Charya, Selenium pollution in the marine environment and marine bacteria in selenium bioremediation, in: M.M. Naik, S.K. Dubey (Eds.), Marine Pollution and Microbial Remediation, Springer, Singapore 2017, pp. 223–237, https://doi.org/10.1007/978-981-10-1044-6_14.

[27] A.A. Kamnev, P.V. Mamchenkova, Yu.A. Dyatlova, A.V. Tugarova, FTIR spectroscopic studies of selenite reduction by cells of the rhizobacterium *Azospirillum brasilense* Sp7 and the formation of selenium nanoparticles, J. Mol. Struct. 1140 (2017) 106–112, https://doi.org/10.1016/j.molstruc.2016.12.003.

[28] K. Lavrinenko, E. Chernousova, E. Gridneva, G. Dubinina, V. Akimov, J. Kuever, A. Lysenko, M. Grabovich, *Azospirillum thiophilum* sp. nov., a diazotrophic bacterium isolated from a sulfide spring, Int. J. Syst. Evol. Microbiol. 60 (12) (2010) 2832–2837, https://doi.org/10.1099/ijs.0.018853-0.

[29] J.M. Day, J. Döbereiner, Physiological aspects of N_2-fixation by a *Spirillum* from *Digitaria* roots, Soil Biol. Biochem. 8 (1) (1976) 45–50, https://doi.org/10.1016/0038-0717(76)90020-1.

[30] A.S. Eswayah, T.J. Smith, A.C. Scheinost, N. Hondow, P.H.E. Gardiner, Microbial transformations of selenite by methane-oxidizing bacteria, Appl. Microbiol. Biotechnol. 101 (17) (2017) 6713–6724, https://doi.org/10.1007/s00253-017-8380-8.

[31] D. Zannoni, F. Borsetti, J.J. Harrison, R.J. Turner, The bacterial response to the chalcogen metalloids Se and Te, Adv. Microb. Physiol. 53 (2007) 1–72, https://doi.org/10.1016/S0065-2911(07)53001-8.
[32] D.C. Nelson, W.H. Casey, J.D. Sison, E.E. Mack, A. Ahmad, J.S. Pollack, Selenium uptake by sulfur-accumulating bacteria, Geochim. Cosmochim. Acta 60 (18) (1996) 3531–3539, https://doi.org/10.1016/0016-7037(96)00221-9.
[33] S. Lampis, E. Zonaro, C. Bertolini, D. Cecconi, F. Monti, M. Micaroni, R.J. Turner, C.S. Butler, G. Vallini, Selenite biotransformation and detoxification by *Stenotrophomonas maltophilia* SeITE02: Novel clues on the route to bacterial biogenesis of selenium nanoparticles, J. Hazard. Mater. 324 (Part A) (2017) 3–14, https://doi.org/10.1016/j.jhazmat.2016.02.035.
[34] R. Jain, N. Jordan, S. Weiss, H. Foerstendorf, K. Heim, R. Kacker, R. Hübner, H. Kramer, E.D. van Hullebusch, F. Farges, P.N.L. Lens, Extracellular polymeric substances govern the surface charge of biogenic elemental selenium nanoparticles, Environ. Sci. Technol. 49 (3) (2015) 1713–1720, https://doi.org/10.1021/es5043063.
[35] E.C. Estevam, S. Griffin, M.J. Nasim, P. Denezhkin, R. Schneider, R. Lilischkis, E. Dominguez-Alvarez, K. Witek, G. Latacz, C. Keck, K.-H. Schäfer, K. Kieć-Kononowicz, J. Handzlik, C. Jacob, Natural selenium particles from *Staphylococcus carnosus*: hazards or particles with particular promise? J. Hazard. Mater. 324 (Part A) (2017) 22–30, https://doi.org/10.1016/j.jhazmat.2016.02.001.
[36] A. Barth, Infrared spectroscopy of proteins, Biochim. Biophys. Acta 1767 (9) (2007) 1073–1101, https://doi.org/10.1016/j.bbabio.2007.06.004.
[37] Z. Movasaghi, S. Rehman, I. ur Rehman, Fourier transform infrared (FTIR) spectroscopy of biological tissues, Appl. Spectrosc. Rev. 43 (2) (2008) 134–179, https://doi.org/10.1080/05704920701829043.
[38] G. Gonzalez-Gil, P.N.L. Lens, P.E. Saikaly, Selenite reduction by anaerobic microbial aggregates: microbial community structure, and proteins associated to the produced selenium spheres, Front. Microbiol. 7 (2016) (Article 571 (14 pp.)) https://doi.org/10.3389/fmicb.2016.00571.
[39] N. Mollania, R. Tayebee, F. Narenji-Sani, An environmentally benign method for the biosynthesis of stable selenium nanoparticles, Res. Chem. Intermed. 42 (5) (2016) 4253–4271, https://doi.org/10.1007/s11164-015-2272-2.
[40] S.I. Yang, G.N. George, J.R. Lawrence, S.G.W. Kaminskyj, J.J. Dynes, B. Lai, I.J. Pickering, Multispecies biofilms transform selenium oxyanions into elemental selenium particles: studies using combined synchrotron X-ray fluorescence imaging and scanning transmission X-ray microscopy, Environ. Sci. Technol. 50 (19) (2016) 10343–10350, https://doi.org/10.1021/acs.est.5b04529.
[41] G. Lucovsky, A. Mooradian, W. Taylor, G.B. Wright, R.C. Keezer, Identification of the fundamental vibrational modes of trigonal, α-monoclinic and amorphous selenium, Solid State Commun. 5 (2) (1967) 113–117, https://doi.org/10.1016/0038-1098(67)90006-3.
[42] O. Van Overschelde, G. Guisbiers, Photo-fragmentation of selenium powder by excimer laser ablation in liquids, Opt. Laser Technol. 73 (2015) 156–161, https://doi.org/10.1016/j.optlastec.2015.04.020.
[43] A.J. Kora, L. Rastogi, Biomimetic synthesis of selenium nanoparticles by *Pseudomonas aeruginosa* ATCC 27853: an approach for conversion of selenite, J. Environ. Manag. 181 (2016) 231–236, https://doi.org/10.1016/j.jenvman.2016.06.029.
[44] H.H. Eysel, S. Sunder, Homonuclear bonds in sulfur-selenium mixed crystals: a Raman spectroscopic study, Inorg. Chem. 18 (9) (1979) 2626–2627, https://doi.org/10.1021/ic50199a059.
[45] M. Vogel, S. Fischer, A. Maffert, R. Hübner, A. Scheinost, C. Franzen, R. Steudtner, Biotransformation and detoxification of selenite by microbial biogenesis of selenium-sulfur nanoparticles, J. Hazard. Mater. (2018)https://doi.org/10.1016/j.jhazmat.2017.10.034.
[46] Leibniz-Institut DSMZ, Deutsche Sammlung von Mikroorganismen und Zellkulturen GmbH, https://www.dsmz.de/catalogues/details/culture/DSM-1843.html.